

THE STRUCTURE OF A TROPICAL CYCLONE SEED AFFECTS ITS PERSISTENCE

Kuan-Yu Lu*¹, Daniel Chavas¹, Danyang Wang¹

¹*Purdue University, West Lafayette, Indiana, USA*

1. INTRODUCTION

Tropical cyclones (TCs) are one of the most devastating natural disasters on Earth. Given that the frequency of TCs – defined as the occurrence counts of TCs within a specified time window and geographical domain – directly controls the overall level of hazard and risk associated with TCs, comprehending the frequency and genesis processes of TCs becomes crucial for predicting and mitigating their impacts (Sobel et al. 2021).

Observational studies have revealed that the majority of TCs originate from pre-existing precursor disturbances, such as the intertropical convergence zone (ITCZ) breakdown (Cao et al. 2013; Kieu and Zhang 2008) or Africa Easterly Waves (AEWs) (Thorncroft and Hodges 2001; Russell et al. 2017). These precursor disturbances are often referred as TC “seeds”. Recent research proposes a seeding-transition framework to interpret TC genesis variability across different climatology (e.g., Hsieh et al. 2020; Vecchi et al. 2019). This framework involves the transformation of a tropical convective cluster into a seed, and the development of a seed into a genesis of TC.

The length of the seeding stage defines the persistence of seeds. If a seed manages to maintain its intensity and encounters a favorable thermodynamic environment (a lower ventilation) before dissipation, it may have a higher chance of undergoing genesis and developing into a TC. In previous studies (Hopsch et al. 2010; Ikehata and Satoh 2021), the main focus has been on the transition probability from seeds to TCs, with relatively less attention given to the duration of the seeding stage. Moreover, past investigations (Lee et al. 2020; Hsieh et al. 2020; Vecchi et al. 2019; Yamada et

al. 2021; Sugi et al. 2020) have primarily concentrated on the influence of environmental factors on seed development, absolute counts, and transition probability. However, there has been limited inquiry into how the structure and dynamics of the seed itself affect its persistence.

Theoretically, seed persistence can affect the frequency of TCs in two ways. First, a seed that persists for a longer duration has a higher probability of encountering an environment favorable for the genesis of TCs, assuming the climatology of the ventilation index remains unchanged. Secondly, increasing the overall persistence of seeds contributes to higher seed counts at any given point during the TC season. Consequently, even if the generation rate remains constant, the annual frequency of TCs may still increase due to the augmented number of seeds. Therefore, investigating the dynamics of seed persistence leads to a more comprehensive understanding of TC frequency.

The meridional variance in the Coriolis parameter on Earth is commonly denoted as β . Recently, Lu and Chavas (2022, hereafter LC22) proposed that the size of a TC-like vortex on a barotropic β -plane is constrained by the vortex Rhines scale. Specifically, circulations larger than the vortex Rhines scale dissipate rapidly due to the influence of planetary Rossby waves, while circulations within the vortex Rhines scale remain largely unaffected and maintain axisymmetry. Note that in this study, the term “planetary Rossby waves” does not refer to Rossby waves that have planetary scale, but specifically to those Rossby waves stimulated by the planetary vorticity gradient, β . LC22’s primary focus was on examining the size of mature TC-like vortices, which typically possess the strongest circulation located well

within the vortex Rhines scale. The impact of planetary Rossby waves on vortex intensity remains uncertain when the strongest circulation of a vortex is situated near or even outside the vortex Rhines scale.

In this study, here we are proposing the following research questions: (1) How do planetary Rossby waves affect the intensity of an individual seed vortex? (2) Does the structure of the vortex affect the vortex intensity response to planetary Rossby waves? To answer these questions, this study will begin by revisiting the Rhines effect as proposed in LC22 and subsequently establish a novel structural parameter to characterize the influence of planetary Rossby waves on vortex intensity.

2. THEORETICAL BACKGROUND

The essence of a TC seed is simply a rotating convective cluster, and its development can be expressed by a barotropic vorticity equation for flow above the boundary layer, away from friction (Hsieh et al. 2020; Raymond and Lopez 2011; Haynes and McIntyre 1987):

$$\frac{d\zeta}{dt} = -\bar{u} \cdot \nabla \zeta - \beta v \quad (1)$$

where ζ represents the relative vertical vorticity, \bar{u} represents the horizontal wind field, $\bar{\zeta}$ is the environmental (background mean) vorticity, β represents the meridional gradient of f , and v is the meridional wind.

When β -term dominates the vorticity tendency in Eq.1, it stimulates planetary Rossby waves. To express the relationship between β -term and the non-linear advection term within a vortex, LC22 defines the ratio between these two terms as the Rhines number, Rh . By converting the coordinate into a cylindrical form, applying scale analysis and β -plane approximation to Eq.1, Rh can be written as follows:

$$\frac{\bar{u} \cdot \nabla \zeta}{\beta v} \equiv Rh = \frac{U_t}{2\pi\beta r^2} \quad (2)$$

where U_t is the tangential circulation speed of a vortex, and r is the radius of the circulation. When a circulation has a faster speed (stronger U_t) or a

smaller size (smaller r), it results in a larger Rh value ($Rh \gg 1$). This indicates that the circulation is not dominated by the β term and can circulate without a significant amount of planetary Rossby wave drag on it. On the other hand, if circulation is slower (has a smaller U_t) or has a larger size (larger r), it results in a smaller Rh value ($Rh \ll 1$), indicating that the circulation is dominated by the β term and is significantly decelerated by planetary Rossby wave drag.

As demonstrated in LC22, we may define the Rhines speed, U_{Rh} , by setting $Rh = 1$ in Eq.(2) and solving for U_t , resulting in:

$$U_{Rh}(r) = 2\pi\beta r^2 \quad (3)$$

For a circulation with a known size, U_{Rh} represents a transition speed that determines the significance of planetary Rossby wave drag. That is, planetary Rossby wave drag is strong when $U_t < U_{Rh}$ and is weak when $U_t > U_{Rh}$. LC22 investigated this theory within the framework of strong mature TC-like vortices where their azimuthally averaged maximum wind speed (V_{max}) is significantly larger than U_{Rh} at the radius of V_{max} (R_{max}), resulting in planetary Rossby wave drag primarily affecting the outer circulation and constraining storm size while maintaining a steady V_{max} .

A seed vortex typically exhibits a lower V_{max} and/or a larger R_{max} . When these conditions are met, the seed's V_{max} is not significantly larger, or can even be smaller than U_{Rh} at R_{max} . As a consequence, the impact of planetary Rossby wave drag on the seed's V_{max} becomes a significant consideration. To precisely quantify the effect of planetary Rossby wave drag on the vortex's intensity, we introduce the concept of vortex structural compactness, denoted as C_v . This structural parameter characterizes the ratio between V_{max} and U_{Rh} at R_{max} :

$$C_v \equiv \frac{V_{max}}{U_{Rh}(@R_{max})} = \frac{V_{max}}{2\pi\beta R_{max}^2} \quad (4)$$

Importantly, C_v varies with both V_{max} and R_{max} . A vortex characterized by a stronger V_{max} and/or a smaller R_{max} has a compact structure ($C_v \gg 1$). On

the other hand, a vortex with a weaker V_{max} and/or a larger R_{max} has an incompact structure ($C_v \ll 1$).

We would like to emphasize that our theory does not provide an explanation for the specific factors influencing a vortex's value of C_v (i.e., how the vortex and its specific structure formed in the first place). Its sole purpose is to describe the impact of planetary Rossby wave drag on the vortex's intensity. Furthermore, the derivation of C_v is based on the barotropic β -plane assumption and does not consider the vorticity source term due to stretching or other factors, as our focus lies in understanding the role of the sink term (planetary Rossby wave drag) acting alone.

Therefore, while C_v directly represents the influence of planetary Rossby wave drag on V_{max} , it cannot solely determine the intensity tendencies of vortices in real-world scenarios.

According to our theory, C_v governs planetary Rossby wave drag on V_{max} , thereby directly influencing the weakening of a vortex due to planetary Rossby wave drag. To investigate the impact of C_v on planetary Rossby wave drag on vortex intensity, as well as its effect on the persistence of TC seed vortex, we propose the following hypothesis: A more compact vortex (a higher C_v) will experience a slower weakening on a barotropic β -plane. We will test this hypothesis by conducting experiments using a barotropic β -plane model. The model will be initialized with both an idealized axisymmetric vortex model and real-world seed vorticity structures obtained from reanalysis data.

3. DATA AND METHODS

3.1 Idealized models

To examine the isolated impact of planetary Rossby wave drag on the vortex intensity, we employ a barotropic β -plane model developed by James Penn and Geoffrey K. Vallis. This model exclusively incorporates planetary Rossby waves as a vorticity sinking process, with no inclusion of any source term. The model utilizes a pseudospectral method to solve Eq.(1) in 2-D space. The model has 500 grid points in

both the x and y directions, with a grid spacing of 20 km. The initial time-step is set at 60 seconds, and the model also employs an adaptive time-step to meet the CFL condition. There is no external forcing applied in any of our experiments. To ensure numerical stability, the model employs a dissipation process known as the high wave-number Smith filter (Smith et al 2002). This filter damps any structures with wave-numbers exceeding 30.

To achieve varying levels of structural compactness while maintaining physical consistency in the generated vortices, we employ idealized wind field models that allow us to systematically modify the V_{max} and R_{max} of an axisymmetric vortex. Firstly, we use the C15 model (Chavas et al 2015) for the complete radial profile of the TC low-level tangential wind field to initialize the barotropic model. The C15 model allows us to define the wind profile using a limited set of storm and environmental parameters. The second idealized wind field model we test is a modified Rankine vortex model. This simplified wind profile model can effectively capture the dynamic characteristics of an actual vortex:

$$U_t(r) = \begin{cases} V_{max} \left(\frac{r}{R_{max}} \right) \left(\frac{R_{max}}{r} \right)^\lambda & \text{when } r < R_{max} \\ V_{max} \left(\frac{r - R_0}{R_{max} - R_0} \right) \left(\frac{R_{max}}{r} \right)^\chi & \text{when } r \geq R_{max} \end{cases} \quad (5)$$

where λ sets the radial increasing rate of tangential winds within R_{max} , χ represents the radial decreasing rate of tangential winds outside R_{max} , and R_0 is the radius of vanishing wind. By adjusting the values of V_{max} and R_{max} within the C15 model and the modified Rankine model and holding other parameters fixed, we can generate tangential wind profiles with varying degrees of C_v .

3.2 TC seeds from reanalysis

The dynamical structure of selected TC seeds is obtained from the European Centre for Medium-range Weather Forecasts (ECMWF) fifth-generation reanalysis data, ERA5. For initializing the barotropic experiments, we arbitrarily selected 20 TC cases, all of which are Category 3, 4, and 5 storms sampled in 2020 and 2021 across all basins. We determine the ending

time and location of each seed track using the corresponding TC's first best track data from the International Best Track Archive for Climate Stewardship, IBTrACS (Knapp et al. 2010). Next, we backtrack the vorticity center of the TC seed hourly for 2 days by identifying the local maximum of relative vorticity at 850hPa in ERA5. A TC seed track is defined when detected vorticity maxima are less than 1.25° apart. To exclude extra-tropical storms, we disregard all tracks located poleward of 30° latitude.

To comprehensively analyze the structure of all TC seeds, which include seeds that never undergo TC genesis, we also adapt a TC seed tracking dataset (Kim and Moon, private communication) that detects and tracks TC seeds in ERA5. Using TempestExtreme (Ullrich et al. 2021), the tracking algorithm first searches for 850-hPa geopotential local minima as centers of candidate seed disturbances and retain only those that satisfy the following conditions: (1) the estimated gradient wind at 500-km from the center exceeds 2 m/s, (2) a local vorticity maximum of magnitude 10^{-5} 1/s or greater exists within 100-km from the center, and (3) relative humidity averaged within 300-km from the center exceeds 75%. The retained centers that are spatially and temporally adjacent are then connected to yield seed disturbance tracks. The duration of the connected seed disturbance should be longer than a day, and one missing time step is allowed in connecting candidates. Additionally, to exclude orographic low-pressure systems, the seed disturbances must be over surface geopotential lower than $980 \text{ m}^2/\text{s}^2$ within a 2° radius for at least a day. The algorithm was applied to 6 hourly ERA5 data in northern hemisphere (Latitude from 0°N to 45°N) with $0.25^\circ \times 0.25^\circ$ horizontal resolution for 1979-2019.

With these TC seed tracks, we can acquire the structure of these seed vortices. The 2-D dynamical structure of a TC seed is defined as the 850hPa relative vorticity within a range of 7.5° from the seed center in both the zonal and meridional directions. Additionally, we only consider the seed's maximum intensity structure to initialize the barotropic model. To exclude adjacent systems, we apply an axisymmetry filter

based on the method proposed by Shimada et al. (2017). The filtered asymmetric vortex can serve as a direct initialization for the barotropic model. Additionally, we can compute the azimuthally averaged vorticity structure to initialize the axisymmetric experimental set. The vorticity profile is also used to determine the V_{max} , R_{max} , and C_v of the seed. When calculating the C_v of a seed, the effective β is used, which includes both planetary β (depends only on latitude) and environmental β (the meridional gradient of the background relative vorticity).

3.3 Barotropic experiment design

We conducted 5 barotropic experiment sets with different initializations. The first experiment set is *VARYRVMAX*, which uses the C15 model to initialize barotropic model (Figure 1a). We systematically vary V_{max} from 10 m/s to 50 m/s with interval of 10 m/s and R_{max} from 100 km to 600 km with interval of 100 km, resulting in 30 TC-like axisymmetric vortices with different C_v values. Each vortex is placed at the center of the domain and simulated separately for a one-day spin-up period. Afterward, β is instantaneously turned on to the constant value for the subsequent 10 days.

The second experiment set is similar to *VARYRVMAX*, but initializing the barotropic model with the modified Rankine model (Figure 1b). This set of experiments is labeled as *RANKINE* and serves to investigate whether the findings from *VARYRVMAX* remain consistent when initializing the barotropic model with a different idealized wind profile model.

The third and fourth experiment set are conducted by initializing the barotropic model with realistic seed vortices obtained from ERA5 reanalysis data. One is denoted as *ASYMSEED*, which utilizes the asymmetric seed vortex directly extracted from ERA5 (Figure 1c). The other one is referred to as *SYMSEED*, in which the vorticity initial conditions of *ASYMSEED* are azimuthally averaged, and the barotropic model is initialized by the axisymmetric vortex with the same configurations as *ASYMSEED* (Figure 1d). vortex with the same configurations as *ASYMSEED*. Note that the azimuthal averaged initial wind profiles of *SYMSEED*

are identical to those in *ASYMSEED*.

The final experiment set is *LARGESEED*, and is conducted by utilizing all axisymmetric members from *SYMSEED* and enlarge their entire structure by a factor of 2 (Figure 1e). The focus of *LARGESEED* is to test the hypothesis by reducing the initial C_v of the

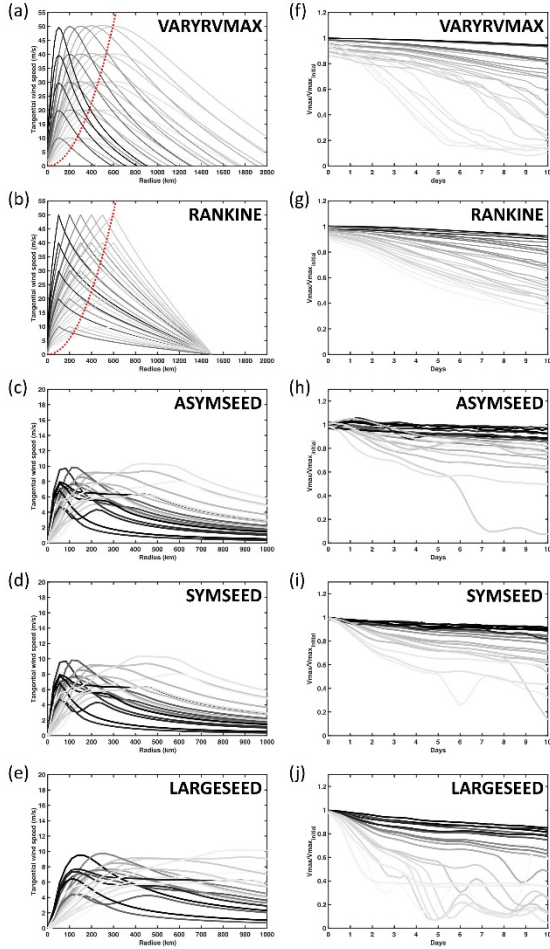


Figure 1. The experiment designs and results of all our experiment sets. (a)-(e) The initial azimuthal averaged tangential wind profiles of all members in *VARYRVMA*, *RANKINE*, *ASYMSEED*, *SYMSEED*, and *LARGESEED*, respectively. (f)-(j) The normalized V_{max} evolution of all members in *VARYRVMA*, *RANKINE*, *ASYMSEED*, *SYMSEED*, and *LARGESEED*, respectively. The gray scale indicates the initial C_v of each member in each experiment set, with darker colors representing relatively higher initial C_v . The red dashed curves in (a) and (b) indicate U_{Rh} profiles on the corresponding β -plane. Note that since all members in *ASYMSEED*, *SYMSEED*, and *LARGESEED* are simulated on different β -planes, their corresponding U_{Rh} profiles are not shown in (c), (d), and (e).

seed while keeping the other aspects of the vortex structure unchanged.

4. RESULTS

4.1 Barotropic experiment sets

Since each member has a different V_{max} evolution, to standardize the comparative analysis across different members, we define the normalized intensity as $\overline{V_{max}} = V_{max}/V_{max,0}$, where $V_{max,0}$ is the initial V_{max} of each member. Figure 1f displays the $\overline{V_{max}}$ evolution for all members in *VARYRVMAX* after turning on the β . All members immediately start weakening after the spin-up period, including the most compact vortex. Overall, more compact vortices exhibit slower rates of weakening. Some less compact vortices are almost entirely dissipated by planetary Rossby wave drag, with $\overline{V_{max}}$ evolution curves fluctuating between 0 and 0.2. Figure 1g shows that, similar as in *VARYRVMAX*, more compact vortices in *RANKINE* weaken slower. While those compact members have similar $\overline{V_{max}}$ evolution across the two experiment sets, less compact vortices in *RANKINE* weaken slower than those in *VARYRVMAX*. Another difference is that there is no member in *RANKINE* that reaches a quasi-steady state during the 10 days of simulation. Results from both *VARYRVMAX* and *RANKINE* support the hypothesis, which states that a more compact vortex will experience less planetary Rossby wave drag on V_{max} and weaken slower. This suggests that our theory is not highly sensitive to the choice of the idealized wind profile model for the initial conditions.

Figure 1h and Figure 1i depict the evolution of $\overline{V_{max}}$ for *ASYMSEED* and *SYMSEED*, respectively. The results obtained from both *ASYMSEED* and *SYMSEED* reveal that more compact vortices experience slower rates of weakening, indicating that our hypothesis is not highly sensitive to the presence of asymmetry in realistic seed vortex structures. They both demonstrate that the initial C_v remains a reliable indicator of how quickly the vortex will weaken due to planetary Rossby wave drag, and the inclusion of 2-D realistic asymmetry does not significantly diminish the reliability of initial C_v . This is of practical use since C_v

can be estimated from V_{max} and R_{max} , and storm central latitude alone.

Finally, Figure 1j illustrates the temporal evolution of $\overline{V_{max}}$ for all members within the *LARGESEED* experiment set. The results from *LARGESEED* provide robust support for our hypothesis, revealing that by manually enlarging the *SYMSEED* members, less compact vortices weaken faster. A comparison between *LARGESEED* and *SYMSEED* demonstrates an overall accelerated weakening rate and more entirely dissipated members in the former.

All barotropic experimental sets presented in this study support our hypothesis that vortices with higher initial C_v values will exhibit slower weakening. To further quantitatively validate this finding, we introduce the weakening rate, denoted as F_{max} , which is defined as the linear regression slope of the $\overline{V_{max}}$ evolution during the first 5 days of the simulation. Figure 2 presents a scatter plot illustrating the relationship

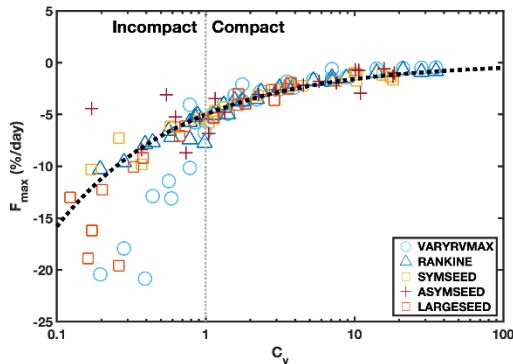


Figure 2 The scatter plot illustrates the relationship between the weakening rate (F_{max}) and the initial structural compactness ($C_{v,0}$) of all members. Members from the same experiment set are indicated by the same marker. The black dashed curve represents the fitted theoretical prediction curve.

between the initial C_v and F_{max} values for all members across all experiment sets.

Overall, a clear positive relationship is observed between the initial C_v ($C_{v,0}$) and F_{max} . Furthermore, it seems that F_{max} is inversely proportional to $-\sqrt{1/C_{v,0}}$. Consequently, an overlay of a fitted prediction curve (indicated by the black dashed curve in Figure 2) highlights the dependence of F_{max} on $C_{v,0}$. This F_{max}

prediction is particularly robust for the compact members across all experimental sets, as evidenced by the close fit of the experimental data to the prediction curve when $C_{v,0} > 1$. However, there are distinct variations among the different experiment sets within those incompact members. These observations suggest that the $C_{v,0} - F_{max}$ relationship is not significantly influenced by structural variance across the experiment sets when the vortex is compact. However, systematic structural differences introduce more variability and decrease the robustness of the F_{max} prediction for the incompact members across all experiment sets.

4.2 Structural differences between developing and non-developing Seeds

The seed dataset comprehensively records every qualified vortex within the tropical region of the Northern Hemisphere, encompassing not only those seeds that ultimately lead to tropical cyclone genesis but also those that dissipate. Therefore, this seed dataset enables us to systematically examine the structural differences between seeds that develop into tropical cyclones and those that do not. Our hypothesis is that: seeds undergoing TC genesis are likely to exhibit a more compact structure.

First, we classified TC seed tracks in the dataset into developing and non-developing seeds based on the maximum 10-meter wind speed. Seed tracks that with a maximum 10-meter wind speed higher than 17.4 m/s for at least 2 timesteps are classified as developing seeds. Others are classified as non-developing seeds. Overall, this dataset documents 1586 developing seeds and 21892 non-developing seeds from 1979 to 2019.

In this study, we are focusing on the difference in structural compactness between developing and non-developing seeds. Since the data set is tracking the local minimum of the geopotential height at 850hPa, we can consider it as the circulation centroid of the seed vortex. Then, we calculate the azimuthally averaged vorticity profile center at the circulation centroid at each timestep of a TC seed track. By

radially integrating the vorticity profile, we can get the azimuthally averaged tangential wind profile of each seed at every timestep. Finally, we identify the inner most local maximum of the tangential wind as V_{max} , and its radius as R_{max} . As for the β , instead of using

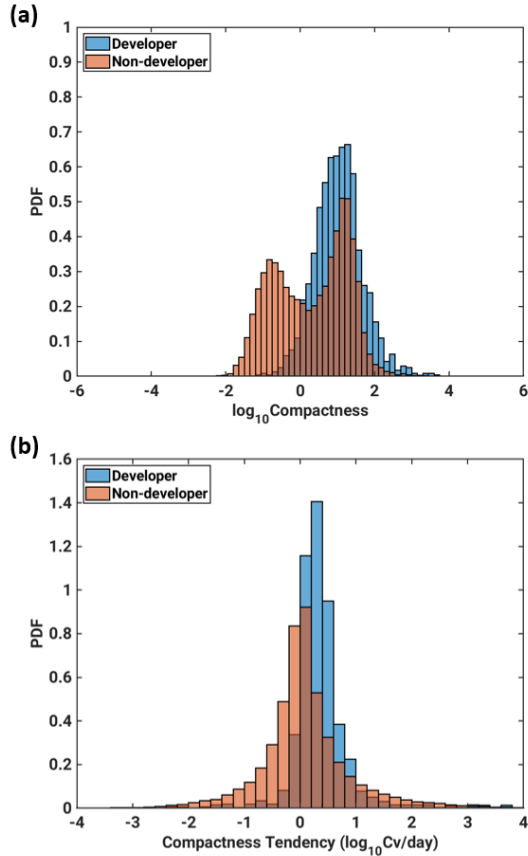


Figure 3. The histograms that demonstrate the structural difference between developing and non-developing seeds. (a) The Probability density function (PDF) of the base 10 logarithm lifetime averaged compactness ($\log_{10} \overline{C_v}$) of all detected TC seeds. Blue bars are PDF for developing seeds, and orange bars are for non-developing seeds. (b) Same as (a), but for the tendency of the base 10 logarithm compactness, which is defined as the slope of the linear regression of $\log_{10} C_v$ time series of a seed.

the planetary β which relies solely on the latitude of the seed vortex center, we employed the effective β that incorporates the environmental vorticity gradient to provide a more nuanced analysis.

Figure 3a demonstrates the normalized distribution of lifetime averaged base 10 logarithm structural compactness ($\log_{10} \overline{C_v}$) of all detected developing and non-developing seeds. The lifetime of a TC seed is

defined as the period beginning with the seed's detection and ending when it either undergoes TC genesis (defined as achieving a maximum 10-meter wind speed exceeding 17.4 m/s) or dissipates. Overall, this result partially supports our hypothesis. Most of the developing seeds have a compact structure ($\log_{10} \overline{C_v} > 0$), only a few of them have an incompact structure. Meanwhile, the quantities of compact and non-compact non-developing seeds are quite similar, with the number of incompact non-developing seeds being only slightly less. Note that the distribution of developing seeds extends further into the positive extreme, indicating a higher prevalence of extremely compact developing seeds compared to non-developing seeds. Also note that most of incompact seeds are non-developing. These results suggest that while it is harder to definitively predict whether a compact seed will undergo TC genesis, a non-compact seed is highly unlikely to develop into a TC.

We also analyze the structural compactness tendency during each TC seed's lifetime. The compactness tendency is defined as the linear regression slope of $\log_{10} C_v$ time series of each TC seed. The compactness tendency of each TC seed is defined as the slope of the linear regression applied to the base 10 logarithmic compactness ($\log_{10} C_v$) time series. Most developing seeds exhibit a positive trend in their compactness evolution, indicating that their structure progressively becomes more compact over time. Only a few developing seeds display a negative compactness tendency. Meanwhile, the compactness tendency of non-developing seeds follows a Gaussian-like distribution centered around zero. These results suggest that a TC seed that is decreasing in compactness is less likely to undergo TC genesis.

5. CONCLUSIONS AND DISCUSSIONS

This study aims to investigate the influence of planetary Rossby wave drag on TC seed vortex intensity and its sensitivity to vortex structure. The following key findings have been established: (1) Vortex structural compactness (C_v) is defined as the ratio between vortex intensity (V_{max}) and the Rhines

speed (U_{Rh}) at the radius of maximum wind (R_{max}), serving as an indicator of planetary Rossby wave drag's impact on V_{max} . (2) Considering planetary Rossby wave drag as the sole vorticity sink, the initial C_v ($C_{v,0}$) of a vortex exhibits a direct correlation with the strength of this wave drag on V_{max} . Hence, $C_{v,0}$ has been established as a reliable predictor of the vortex weakening rate (F_{max}) induced by planetary Rossby wave drag. (3) The weakening rate in our experiments closely follows a $-\sqrt{1/C_{v,0}}$ dependence, and is particularly robust when the vortex is initially compact. (4) Structurally incompact TC seeds in the ERA5 dataset are significantly less likely to undergo TC genesis. (5) TC seeds in the ERA5 dataset exhibiting a negative trend in compactness are less likely to undergo TC genesis.

Across all of our experiment sets, even when a vortex possesses a C_v value greater than 1, it still experiences weakening due to planetary Rossby wave drag. This observation underscores the fact that planetary Rossby waves can be stimulated even when the circulation is within the dynamical pouch. However, due to the relatively short circulation timescale, the vortex's compact circulation is able to self-advect before being significantly affected by planetary Rossby wave drag, resulting in less weakening. Consequently, if a vortex exhibits a C_v value that is not significantly larger than 1, self-advection at R_{max} is comparable in magnitude to planetary Rossby wave drag, albeit slightly greater. As a result, the vortex will weaken due to planetary Rossby wave drag, while the weakening rate is much slower than those incompact vortices ($C_v < 1$).

Our statistical analyses of the TC seed dataset suggest that while structural compactness alone is not an effective indicator for distinguishing developing cases among compact seeds, incompact seeds are significantly less likely to undergo TC genesis. This observation is closely tied to the physical definition of structural compactness, which characterizes the impact of planetary Rossby wave drag on vortex intensity—a weakening mechanism. Therefore, although compact seeds experience less planetary

Rossby wave drag, this alone does not provide information about the presence of a vorticity source necessary for intensification, which is essential for the TC genesis process. Conversely, a less compact seed is subject to considerably greater planetary Rossby wave drag affecting its intensity, and our findings indicate that this factor is so predominant that the majority of these incompact seeds are unable to initiate TC genesis. Future investigations should concentrate on identifying parameters that can effectively distinguish between developing and non-developing compact seeds.

The parameter C_v proposed in this study has important practical applications, particularly in the context of TC seed dynamics on Earth. It plays a crucial role in determining a seed vortex's ability to resist significant drag by planetary Rossby waves, especially in the tropics. The requirement to maintain compactness in the seed vortex imposes limitations on its representation in weather and climate modeling. For instance, when employing a global model with coarser horizontal resolution, the smaller values of R_{max} and stronger magnitudes of V_{max} associated with a compact seed vortex may not be adequately resolved. Consequently, the model might underestimate the seed's C_v , leading to an overestimation of planetary Rossby wave drag and predicting a faster weakening for the seed. This may explain why lower resolution models tend to produce far fewer tropical cyclones than observed (Yamada et al. 2021; Sobel et al. 2021; Roberts et al. 2020; Murakami and Sugi 2010). Ensuring accurate representation of compactness becomes essential in such modeling scenarios to obtain reliable predictions for TC seed evolution.

While we utilize a realistic TC seed structure obtained from ERA5 to initialize our barotropic model and examine the rate of vortex weakening, it is important to note that our results do not directly represent the actual V_{max} evolution of the seed in reanalysis data. The parameter C_v , as demonstrated in the preceding section, solely captures the influence of planetary Rossby wave drag on V_{max} , disregarding other physical processes, particularly the vorticity

source term due to vortex stretching from convection (Hsieh et al. 2020), that may potentially impact vortex intensity. Future work seeking to understand TC seeds in the real world should examine the competing effects of both source and sink terms of vorticity.

Several aspects of this subject remain unresolved, warranting further investigation. While our theory and experimental results indicate the importance of C_v as a parameter for examining the evolution of vortex intensity, the factors governing the evolution of vortex structural compactness remain uncertain. The underlying causes behind the comparatively less robust prediction of F_{max} for incompact vortices remain uncertain. Further exploration is needed to delve into the potential influence of other variations in vortex structure on this phenomenon. Additionally, since this study only investigated the structure of developing seeds, it remains uncertain whether non-developing seeds statistically possess a less compact structure compared to developing seeds. Addressing these questions requires modeling the development of TC seeds and conducting a comprehensive survey that includes both developing and non-developing seeds to better understand the interplay between TC seed structure and intensity. By investigating these aspects, we can gain deeper insights into the dynamics and behavior of TC seeds, which may lead to advancements in our understanding of TC genesis and frequency.

References

- Cao, X., Chen, G. and Chen, W. (2013), Tropical cyclogenesis induced by ITCZ breakdown in association with synoptic wave train over the western North Pacific. *Atmos. Sci. Lett.*, 14: 294-300.
- Chavas, D. R., N. Lin, and K. Emanuel, 2015: A Model for the Complete Radial Structure of the Tropical Cyclone Wind Field. Part I: Comparison with Observed Structure. *J. Atmos. Sci.*, 72, 3647–3662.
- Haynes, P. H., and M. E. McIntyre, 1987: On the Evolution of Vorticity and Potential Vorticity in the Presence of Diabatic Heating and Frictional or Other Forces. *J. Atmos. Sci.*, 44, 828–841.
- Hopsch, S. B., C. D. Thorncroft, and K. R. Tyle, 2010: Analysis of African Easterly Wave Structures and Their Role in Influencing Tropical Cyclogenesis. *Mon. Wea. Rev.*, 138, 1399–1419.
- Hsieh, T.L., Vecchi, G.A., Yang, W. et al. Large-scale control on the frequency of tropical cyclones and seeds: a consistent relationship across a hierarchy of global atmospheric models. *Clim Dyn* 55, 3177–3196 (2020).
- Ikehata, K., & Satoh, M. (2021). Climatology of tropical cyclone seed frequency and survival rate in tropical cyclones. *Geophysical Research Letters*, 48, e2021GL093626.
- Kieu, C. Q., and D. Zhang, 2008: Genesis of Tropical Storm Eugene (2005) from Merging Vortices Associated with ITCZ Breakdowns. Part I: Observational and Modeling Analyses. *J. Atmos. Sci.*, 65, 3419–3439.
- Knapp, K. R., M. C. Kruk, D. H. Levinson, H. J. Diamond, and C. J. Neumann, 2010: The International Best Track Archive for Climate Stewardship (IBTrACS). *Bull. Amer. Meteor. Soc.*, 91, 363–376.
- Lee, C., S. J. Camargo, A. H. Sobel, and M. K. Tippett, 2020: Statistical–Dynamical Downscaling Projections of Tropical Cyclone Activity in a Warming Climate: Two Diverging Genesis Scenarios. *J. Climate*, 33, 4815–4834.
- Lu, K., and D. R. Chavas, 2022: Tropical Cyclone Size Is Strongly Limited by the Rhines Scale: Experiments with a Barotropic Model. *J. Atmos. Sci.*, 79, 2109–2124.
- Murakami, H., and M. Sugi, 2010: Effect of model resolution on tropical cyclone climate projections. *SOLA*, 6, 73–76.
- Raymond, D. J. and López Carrillo, C.: The vorticity budget of developing typhoon Nuri (2008), *Atmos. Chem. Phys.*, 11, 147–163.
- Roberts, M. J., and Coauthors, 2020: Impact of Model Resolution on Tropical Cyclone Simulation Using the HighResMIP–PRIMAVERA Multimodel Ensemble. *J. Climate*, 33, 2557–2583.
- Russell, J. O., A. Aiyyer, J. D. White, and W. Hannah (2017), Revisiting the connection between African Easterly Waves and Atlantic tropical cyclogenesis, *Geophys. Res. Lett.*, 44, 587–595.

Sobel, A. H., Wing, A. A., Camargo, S. J., Patricola, C. M., Vecchi, G. A., Lee, C.-Y., & Tippett, M. K. (2021). Tropical cyclone frequency. *Earth's Future*, 9, e2021EF002275.

Shimada, U., K. Aonashi, and Y. Miyamoto, 2017: Tropical Cyclone Intensity Change and Axisymmetry Deduced from GSMaP. *Mon. Wea. Rev.*, 145, 1003–1017.

Smith, K. S., G. Boccaletti, C. C. Henning, I. Marinov, C. Y. Tam, I. M. Held, and G. K. Vallis, 2002: Turbulent diffusion in the geostrophic inverse cascade. *Journal of Fluid Mechanics*, 469, 13–48.

Sugi, M., Y. Yamada, K. Yoshida, R. Mizuta, M. Nakano, C. Kodama, and M. Satoh, 2020: Future changes in the global frequency of tropical cyclone seeds. *SOLA*, 16 (0), 70–74.

Thorncroft, C., and K. Hodges, 2001: African Easterly Wave Variability and Its Relationship to Atlantic Tropical Cyclone Activity. *J. Climate*, 14, 1166–1179.

Ullrich, P., C. Zarzycki, E. E. McLenny, M. C. Pinheiro, A. M. Stansfield, and K. A. Reed, 2021: TempestExtremes v2.1: A community framework for feature detection, tracking and analysis in large datasets. *Geosci. Model Dev.*, 14, 5023–5048.

Vecchi, G.A., Delworth, T.L., Murakami, H. et al. Tropical cyclone sensitivities to CO₂ doubling: roles of atmospheric resolution, synoptic variability and background climate changes. *Clim Dyn* 53, 5999–6033 (2019).

Yamada, Y., Kodama, C., Satoh, M. et al. Evaluation of the contribution of tropical cyclone seeds to changes in tropical cyclone frequency due to global warming in high-resolution multi-model ensemble simulations. *Prog Earth Planet Sci* 8, 11 (2021).